JOURNAL OF CATALYSIS 146, 218–227 (1994)

Molybdenum Nitride Catalysts

I. Influence of the Synthesis Factors on Structural Properties

Jeong-Gil Choi, Rane L. Curl, and Levi T. Thompson[1]

Department of Chemical Engineering, The University of Michigan, Ann Arbor, Michigan 48109-2136

Received April 6, 1993; revised September 29, 1993

Effects of the synthesis parameters on the structural properties of molybdenum nitride catalysts, prepared by the temperature-programmed reaction of MoO_3 with NH_3, have been examined. Molybdenum trioxide was heated in flowing NH_3 through two linear heating segments (623 to 723 K then 723 to 973 K) with different space velocities in a 2^3 factorial design. The temperature limits for these heating segments were defined based on the results of *in situ* X-ray diffraction analysis of the gas–solid reaction. The resulting catalysts were characterized using BET surface area analysis, environmental scanning electron microscopy, *ex situ* X-ray diffraction, and oxygen chemisorption. The primary bulk phase present was γ-Mo_2N. Some of the lower surface area catalysts also contained MoO_2 and Mo, but there was no evidence of nitrides other than γ-Mo_2N. The catalysts consisted of micrometer-sized, plate-like aggregates of nanometer-sized crystallites, and possessed surface areas ranging up to $\approx$140 m^2/g depending on the synthesis and reduction conditions employed. Statistical analysis of the results revealed that the space velocity individually and the heating rates combined had the most significant effects on the structural properties. The production of catalysts with surface areas in excess of 50 m^2/g required the use of slow heating rates during the first segment and high space velocities. We concluded that the key to producing the highest surface area Mo nitrides was channeling the reaction through H_xMoO_3 ($x \leq 0.34$) and γ-$Mo_2O_yN_{1-y}$ intermediates. Passivation of the materials immediately following synthesis appeared to produce an oxynitride at the surface. Reduction of the passivated materials in H_2 at temperatures up to 673 K caused a significant increase in the surface area and O_2 uptake. The O_2 uptake for the low and medium surface area catalysts varied linearly with the BET surface area and corresponded to an O:Mo stoichiometry of approximately 1:5. The oxygen site density for the highest surface area nitride was lower than those for the lower surface area catalysts, presumably due to differing surface structures.

INTRODUCTION

Molybdenum nitrides are effective and selective hydrotreatment catalysts (1–4). The use of these materials as commercial catalysts warrants their production with high surface area to volume ratios. There are several ways to achieve high surface areas: generating the bulk material in a porous form, producing nanostructured powders, or dispersing the active species on high surface area supports. Volpe *et al.* (5) reported that high surface area unsupported molybdenum nitrides can be prepared by reacting MoO_3 with NH_3 while heating linearly in a temperature programmed manner. The properties of the resulting materials appear to be strongly dependent on the synthesis conditions employed. Table 1 lists surface areas of selected molybdenum nitrides produced via the temperature-programmed reaction (TPR) of MoO_3 with NH_3. While correlations between the heating rates, space velocities and surface areas are not clear, use of the temperature program with two heating segments led to the production of molybdenum nitrides with surface areas greater than 150 m^2/g.

Volpe and Boudart (8) concluded that the high surface areas were a consequence of MoO_3 being nitrided through a series of topotactic reactions. Topotactic solid-state reactions are those in which the product is formed in crystallographically equivalent orientations relative to the parent crystal (9). The gross morphology of the parent material is typically maintained during topotactic transformations. Since the molybdenum nitrides are much denser than the molybdenum oxides, this type of reaction would result in the creation of cracks and the development of high surface areas. It has been suggested that slow heating rates during the early stages of the reaction avoid sintering of the intermediates, and high space velocities mitigate hydrothermal sintering during the latter stages of the reaction (8). No explanation has been offered for the use of fast heating rates during the latter stage of the reaction. Jaggers *et al.* (7) stressed the importance of the reaction intermediates in determining the surface areas and phase constituents. They suggested that the solid-state reaction of MoO_3 with NH_3 proceeds through two parallel reaction pathways: $MoO_3 \rightarrow MoO_xN_{1-x} \rightarrow \gamma$-$Mo_2N$ and $MoO_3 \rightarrow MoO_2 \rightarrow \gamma$-$Mo_2N$ + δ-MoN. Formation of the oxynitride,

[1] To whom correspondence should be addressed.

0021-9517/94 $6.00

TABLE 1

Examples of Previous Results for the Synthesis of Molybdenum Nitrides

Surface area (m^2/g)	T_{onset} (K)	T_{final} (K)	Heating rate (K/hr)	Space velocity (hr^{-1})	Reference
22	≈550[a]	≈1050	61	10	(6)
54	RT	980	36	15	(2)
57	298	1050	36	380	(7)
88	≈550[a]	≈1050	90	48	(6)
102	RT	980	36	76	(2)
190	690[a,b]	740	36	36	(5)
	740	979	180		

[a] Solid reactant quickly heated from room temperature, RT, to T_{onset} in NH_3.

[b] Solid reactant heated through two linear heating segments.

MoO_xN_{1-x}, resulted in a large increase in surface area due to the pseudomorphic nature of the reaction while the formation of MoO_2 led to lower surface area materials. It was also concluded that the temperature at which the oxynitride intermediate reacted determined the phase of the nitride produced, however, the effects of the heating rate on the reaction selectivities and resulting surface areas were not studied.

For processes involving parallel solid-state reactions, one would expect the product selectivity to be a function of the heating rate much the way the selectivity for multiple chemical reactions is a function of temperature. Consider, for example, the TPR of plate-like solid particles with a gaseous reactant under conditions where the solid-state reactions are rate controlling. This process can be modeled as

$$d\chi/dt = k_T(1-\chi)^n f(P), \qquad [1]$$

where χ is the fractional conversion, k_T is the rate constant at temperature T, and $f(P)$ characterizes the functional relationship between the reaction rate and gas-phase reactant partial pressure. Substituting for the rate constant and the relationship between time and temperature results in the expression

$$d\chi/(1-\chi)^n = Ae^{-E/RT}f(P)dT/\beta, \qquad [2]$$

where A is the preexponential factor, E is the apparent activation energy, R is the gas constant, and β is the heating rate. For a reaction that is first order with respect to the solid reactant under conditions where the gas-phase concentration is essentially constant (differential conditions), the conversion would be an exponential function of the inverse of the heating rate. For a network of parallel first-order reactions the selectivity to product A, Y_A, would be a function of the heating rate,

$$Y_A = e^{-\kappa_A/\beta} \Big/ \sum_j e^{-\kappa_j/\beta}, \qquad [3]$$

where $\kappa_j = Rf_j(P)(k_{T_f} - k_{T_i})_j/E_j$ is characteristic of the reaction leading to product j, and T_f and T_i are the final and initial temperatures, respectively. Expressions for reactions of different orders and processes controlled by other elementary steps (i.e., transport of reactants) can also be derived. In each case the product selectivity is expected to be a function of the heating rate.

The purpose of research described in this paper was to systematically evaluate the influence of the heating rates and space velocities on the structural properties of molybdenum nitride catalysts prepared using the TPR method. The experiments were devised using a standard factorial design, and the properties that were evaluated included the BET surface area, phase constituents, crystallite size, and chemisorptive uptake. An additional goal was to provide some information concerning the effects that reduction in H_2 have on the properties of the molybdenum nitrides. The hydrodenitrogenation activities and selectivities of these catalysts in the absence and presence of H_2S will be described in a follow-up paper (10).

EXPERIMENTAL

Synthesis

Reports in the literature indicate that the nitridation of MoO_3 with NH_3 occurs in two steps (7, 8), therefore a two-segment heating program was used to synthesize the molybdenum nitrides. We used *in situ* XRD analysis to define the temperature intervals during which the transformations occurred. The heating rates employed were selected to bracket those used by others. The temperature at which the first crystalline products were formed during the TPR of MoO_3 with NH_3 increased with increasing heating rate, suggesting kinetic rather than thermodynamic control. In each case the first crystalline product was H_xMoO_3 ($x \leq 0.34$) or MoO_2. For heating rates near 100 K/hr, the highest heating rate employed during the first heating segment, MoO_3 reacted at ≈700 K. Evidence of H_xMoO_3 was detected starting at ≈673 K using a heating rate of 40 K/hr. The nitridation of MoO_3 was complete by 950 K for heating rates less than or equal to 200 K/hr, the highest heating rate employed in our study. Given these results, the time–temperature program illustrated in Fig. 1 was devised.

We employed a factorial design to evaluate the influence of the two heating rates and the space velocity on the product properties. Two levels for each of the three vari-

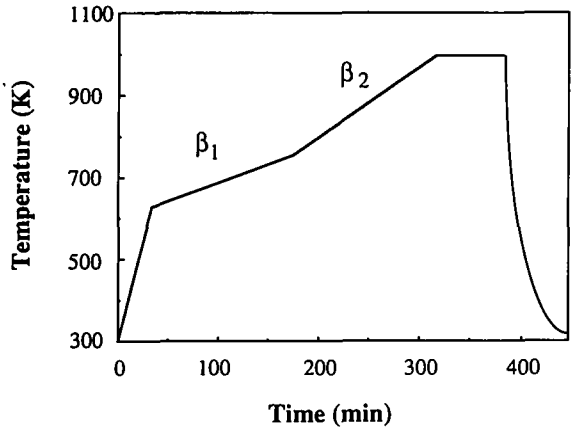

FIG. 1. Schematic of the temperature versus time schedule used during the temperature-programmed reaction of MoO_3 with NH_3.

ables were investigated, requiring 2^3 experiments. The intent of this study was only to screen for the effects and their interactions, therefore, the experiments were not replicated. This experimental design has been described elsewhere along with methods for analysis of the effects (11).

The synthesis reactor was a 0.625-in.-o.d. quartz tube fitted with a water jacket to cool the effluent gases. The reactor section was placed inside the furnace (Thermcraft Model 132), and the temperature was monitored using a chromel–alumel thermocouple and controlled by a programmable temperature controller (Omega Series CN-2010). Only prepurified gases were employed and they were passed through traps to ensure purity. Helium (Air Products, 99.995%) was used after removing residual O_2 and H_2O using an oxytrap (Matheson Model 6406). Any moisture was removed from the NH_3 (Scott, 99.998%) using a bed of BaO (Aldrich, 90%). The gas flow rates were measured using rotameters and a bubble flow meter, and controlled using needle valves.

In a typical experiment, MoO_3 powder (Alfa, 99.95%, 0.9 m^2/g) was placed in the reactor on a quartz wool plug. The reaction temperature was quickly increased from room temperature to 623 K over 0.5 hr, from 623 to 723 K at 40 or 100 K/hr (β_1), and finally from 723 to 973 K at 100 or 200 K/hr (β_2). The temperature was maintained at 973 K for an additional hour before the product was rapidly cooled to room temperature in flowing NH_3. The molar hourly space velocities (SV) of 8.5 or 17 mole NH_3/mole MoO_3/hr were selected to approximate those used by others while yielding sufficient amounts of product for characterization. After synthesis, the cooled product was purged with He for 10 min. High surface area Mo nitrides tend to be pyrophoric; therefore, the materials were passivated for 2 hr in a mixture of 0.996% O_2 in He flowing at 20 cm^3/min, then removed from the reactor. Prior to determination of their surface areas and chemisorptive capacities, the passivated materials were reduced in H_2 at temperatures up to 673 K.

Additional syntheses were performed using H_xMoO_3 ($x \leq 0.34$) and MoO_2 (Alfa, 99%) as reactants. The H_xMoO_3 was synthesized by the reduction of MoO_3 with HCl and zinc metal powder as originally described by Glemser and Lutz (12) or by the temperature programmed reduction of MoO_3 with flowing H_2 (quickly heated from room temperature to 623 then to 723 K at 100 K/hr, followed by a soak at 723 K for 1 hr).

Characterization

BET surface areas and oxygen chemisorption were measured before and after reduction in H_2 using a Quantasorb Model QS-17 sorption analyzer. A gas mixture containing 29.3% N_2 in He was used for standard single point BET surface area measurements. For the chemisorption measurements, calibrated volumes of 9.98% O_2 in He were pulsed over the catalysts at 195 K until the surface was saturated. The BET surface areas and O_2 uptakes were very reproducible, and the averaged values are reported.

A computer controlled Rigaku Rotaflex DMAX-B rotating anode X-ray diffractometer was used for bulk characterization of the Mo nitrides. *In situ* high temperature X-ray diffraction was carried out using a computer controlled Rigaku Geigerflex DMAX-B sealed tube diffractometer. The sizes and shapes of particles on the surfaces of the Mo nitrides were examined using an ElectroScan Model E3 Environmental Scanning Electron Microscope (ESEM). The ESEM differs from a standard scanning electron microscope in that images can be collected in an environment of up to 20 Torr of a gas with an adequate ionization potential. Thus ESEM permits the *in situ* investigation of reacting materials and the examination of uncoated specimens. Gases that are suitable for ESEM include H_2O, NH_3, and H_2. The micrographs presented here are of the passivated materials taken at room temperature using NH_3 as the imaging gas.

RESULTS

Bulk Structure/Surface Morphology

The primary crystalline phase produced during the TPR of MoO_3 with NH_3 was γ-Mo_2N as determined by X-ray diffraction. While the equilibrium phases expected under the conditions used in this work include γ-Mo_2N, β-$Mo_{16}N_7$, and δ-MoN (13, 14), there was no evidence of the production of β-$Mo_{16}N_7$ or δ-MoN. As indicated in Table 2, MoO_2 and Mo were also detected in some of the materials.

TABLE 2

Bulk Structural Properties of the Molybdenum Nitrides

Catalyst code	Phases present	Crystallite size (nm)	$I(200)/I(111)$
MoN-1	γ-Mo_2N	10	0.6
MoN-2	γ-Mo_2N	8	2.9
MoN-3	γ-Mo_2N	11	0.8
	MoO_2	45	
MoN-4	γ-Mo_2N	13	1.1
MoN-5	γ-Mo_2N	8	0.6
	Mo	28	
MoN-6	γ-Mo_2N	14	0.8
MoN-7	γ-Mo_2N	13	0.7
MoN-8	γ-Mo_2N	8	0.7
	Mo	27	
γ-Mo_2N[a]	γ-Mo_2N		0.5

[a] From the Powder Diffraction File (16).

The crystallite dimensions were determined using the Scherrer equation (15),

$$D_{\langle hkl\rangle} = 0.9\lambda/(B\cos\theta), \qquad [4]$$

where $D_{\langle hkl\rangle}$ is the crystal thickness in the $\langle hkl\rangle$ direction, λ is the wavelength of the X-radiation, B is the peak width corrected for instrumental broadening, and θ is the Bragg angle of the diffraction peak. For most of the molybdenum nitrides, the crystal thicknesses in the $\langle 200\rangle$ and $\langle 111\rangle$ directions were within experimental error of each other. The two lowest surface area catalysts (i.e., MoN-5 and MoN-8) were notable exceptions. For these materials, $D_{\langle 200\rangle}$ was greater than $D_{\langle 111\rangle}$ suggesting that the crystallites were plate-like or rod-like extending out in the $\langle 100\rangle$ direction. The crystallite size was taken as the average of $D_{\langle 200\rangle}$ and $D_{\langle 111\rangle}$. While the γ-Mo_2N crystallite sizes varied, there was no apparent correlation between the crystallite size and synthesis conditions.

There was a significant degree of texturing in the high surface area catalysts (i.e., MoN-2 and MoN-4). A semi-quantitative measure of texturing or preferential orientation is the relative intensity of peaks in the diffraction pattern. Here we used the ratio of the intensities of the (200) and (111) reflections, $I(200)/I(111)$, as a measure of the texturing. The $I(200)/I(111)$ for the two highest surface area materials were much greater than 0.5, the value expected for randomly distributed γ-Mo_2N crystallites of uniform dimensions (16). This preferential orientation remained after grinding and suggested alignment of the crystallites in the $\langle 100\rangle$ direction. This type of texturing, which is characteristic of high surface area Mo nitrides (2, 8), was probably a consequence of the pseudomorphic nitridation of the MoO_3 particles into γ-Mo_2N.

The passivated Mo nitrides contained micron-sized, plate-like and rod-like aggregates of much smaller, nanometer-sized particles. Except for the low surface area catalysts, the average sizes of these smaller particles were consistent with those estimated from the BET surface areas assuming spherical particles (see Table 3). The crystallite sizes for the low surface area materials were more consistent with the particles being plate-like.

There were other subtle differences between the characters of the Mo nitrides. Figures 2 and 3 compare the morphologies of the lowest (MoN-8) and highest surface area (MoN-2) materials, respectively. The predominance of large plate-like particles increased with increasing surface area of the catalyst. Furthermore, while the morphologies of all of the nitrides resembled that of the precursor, MoN-2 bore the greatest resemblance to the MoO_3 (Fig. 4). The large MoO_3 particles did not, however, appear to contain smaller particles as we observed for the molybdenum nitrides. These results suggested that, to varying degrees, the reaction of MoO_3 to γ-Mo_2N was pseudomorphic for all of the materials. The significant increase in the density on going from MoO_3 (4.69 g/cm^3) to γ-Mo_2N (9.4 g/cm^3) would result in the evolution of cracks, and the development of significant amounts of internal surface area.

Effect of Hydrogen Reduction on Surface Area

It has been reported that the passivation of molybdenum nitrides causes a loss in surface area and chemisorption capacity (5). Prior to use as catalysts, the passivated nitrides are usually pretreated. The passivation layer is often removed via reduction of the material in H_2. Little is known about the character of the passivation layer and the product formed at the surface after reduction.

The response of the materials to reduction in H_2 at varying temperatures and times was characteristic of an activated solid-state reaction. The catalysts were reduced in flowing H_2 at temperatures between 473 and 673 K for up to 10 hr then purged with flowing He at the reduction temperature before being cooled to room temperature. The effects of reduction temperature and time on the BET surface areas and oxygen uptakes are given for MoN-1 (a low surface area material) and MoN-2 (the highest surface area material). The initial surface areas were measured following treatment in He at 400°C for 4 hr (19.8 and 58.9 m^2/g for MoN-1 and MoN-2, respectively). As the H_2 reduction temperature was increased, the surface area increased monotonically (Fig. 5). As the reduction time at 673 K was increased, the BET surface area increased to a maximum after 3–5 hr then remained constant within experimental error (Fig. 6). The total surface area was increased by almost a factor of 2 depending on the initial properties of the material and the reduction conditions.

TABLE 3

Effect of Synthesis Factors on Properties of the Molybdenum Nitrides

Catalyst code	Heating rate (K/hr) β_1	Heating rate (K/hr) β_2	Space velocity (hr^{-1})	Preparation code	Surface area (m^2/g)	Particle size[a] (nm)	O_2 uptake (μmole/g)
MoN-1	100	200	17	+++	24	27	67
MoN-2	40	200	17	−++	116	6	112
MoN-3	100	100	17	+−+	44	15	85
MoN-4	40	100	17	−−+	52	12	93
MoN-5	100	200	8.5	++−	12	53	24
MoN-6	40	200	8.5	−+−	28	23	54
MoN-7	100	100	8.5	+−−	39	14	58
MoN-8	40	100	8.5	−−−	4	160	7

[a] Estimated from the surface areas assuming spherical particles.

The highest surface area observed was 138 m^2/g for MoN-2 following H_2 reduction at 673 K for 4 hr.

As the gross dimensions of the Mo nitride particles did not change, the results indicated that the near surface density increased on reduction in H_2. It has been suggested that during passivation oxygen is chemisorbed on the nitride surface, a one to two monolayer thick oxide layer is formed, or oxygen diffuses into the lattice forming an oxynitride (2, 6). Removal of chemisorbed oxygen would not cause a change in the surface area. Given its limited spatial extent, the reduction of a monolayer thick oxide would not result in a significant increase in the surface area. Furthermore, oxygen in amounts exceeding that expected for a monolayer were removed from the passivated Mo nitrides during temperature programmed reduction (17). A plausible explanation for the increase in surface area following reduction is that the region near the surface was expanded due to the presence of oxygen in the lattice. On reduction this oxygen was removed yielding a denser structure and higher surface area. Both the γ-Mo_2N and β-$Mo_{16}N_7$ lattices are capable of accommodating additional nitrogen or oxygen (the radius of oxygen satisfies the Hägg rule for Mo compounds). We have therefore concluded that passivation generates an oxynitride from which oxygen is removed during reduction in H_2. A similar conclusion was drawn based on the results

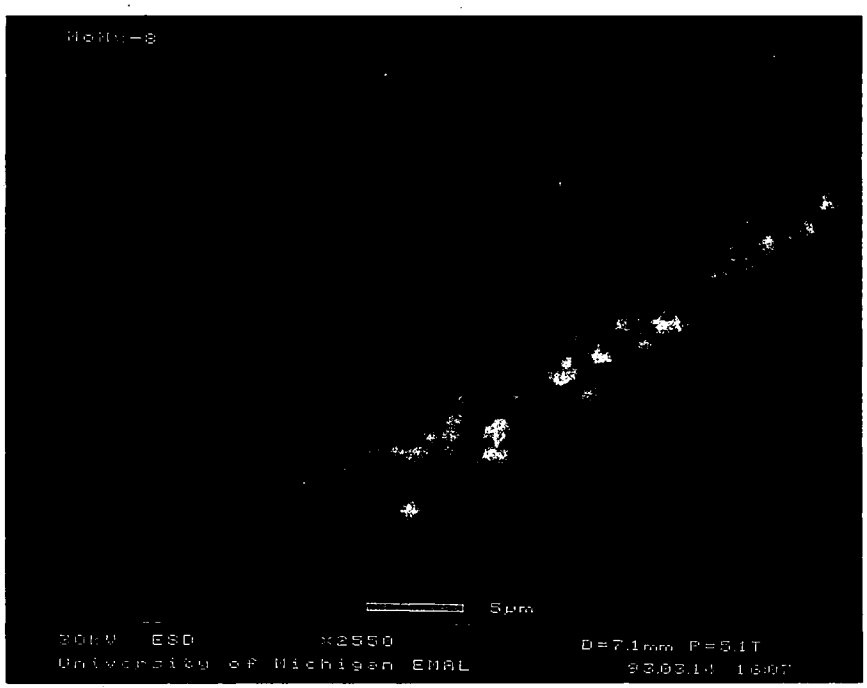

FIG. 2. Environmental scanning electron micrograph of the lowest surface area molybdenum nitride (MoN-8) taken under 5.1 Torr of NH_3.

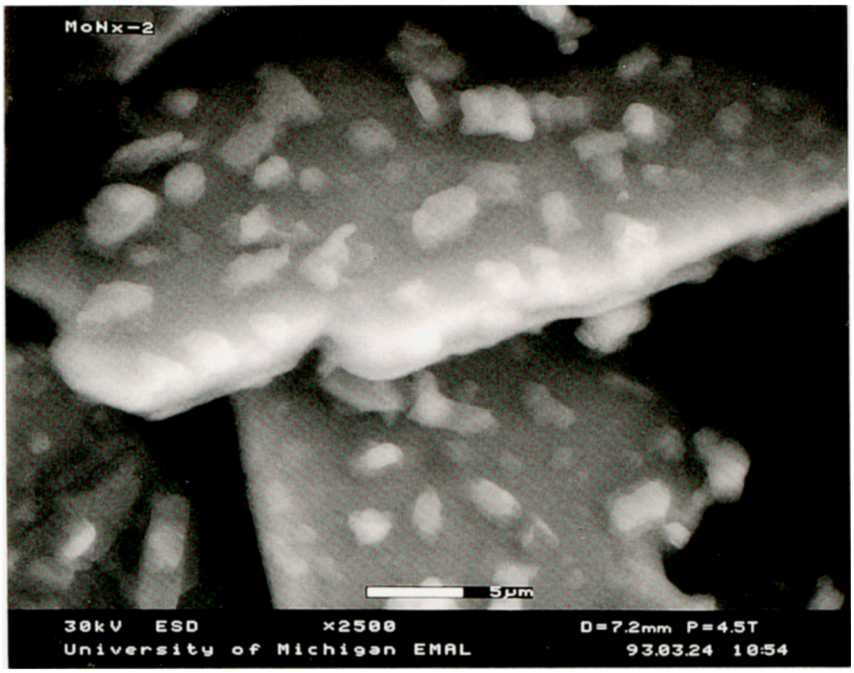

FIG. 3. Environmental scanning electron micrograph of the highest surface area molybdenum nitride (MoN-2) taken under 4.5 Torr of NH_3.

of a high resolution transmission electron microscopic investigation (18).

Effects of Heating Rates and Space Velocity on Surface Area/O_2 Chemisorption

Surface areas of the catalysts following reduction in flowing H_2 at 673 K for 3 hr are summarized in Table 3. The average particle size, D_p, was calculated using the equation

$$D_p = f_p/S_g\rho, \qquad [5]$$

where f_p is characteristic of the particle shape ($f_p = 6$ for spheres and cubes, $f_p = 4$ for cylinders, and $f_p = 2$ for

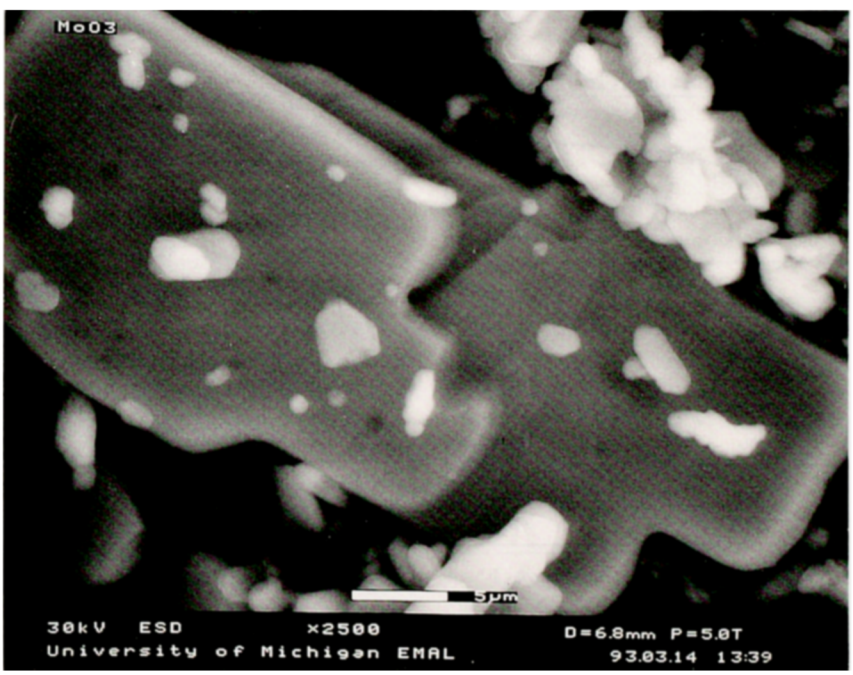

FIG. 4. Environmental scanning electron micrograph of the MoO_3 powder used to synthesize the Mo nitrides. The powder was examined under 5.0 Torr of NH_3.

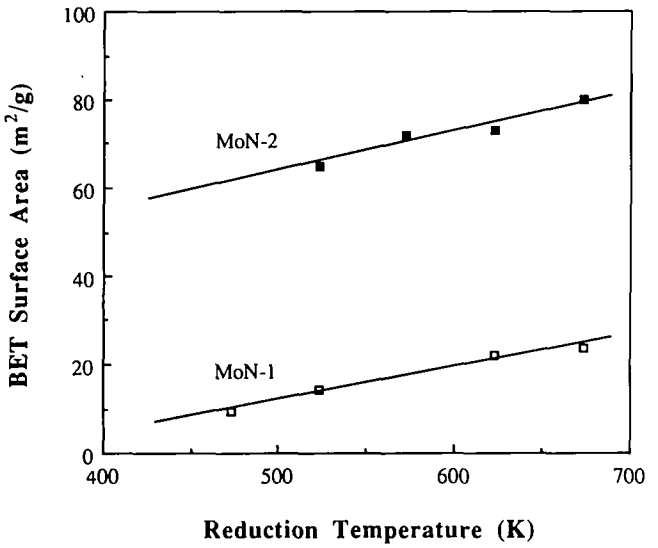

FIG. 5. Effect of reduction temperature on the BET surface areas of MoN-1 and MoN-2. These materials were reduced in H_2 for 1 hr prior to the surface area measurements.

plates), S_g is the surface area, and ρ is the density of the material (here taken to be 9.4 g/cm^3 for γ-Mo_2N). This relationship holds when the individual particles are nonporous (19). As is standard in factorial design, we represented the two levels of each synthesis factor as "+" for the high level and "−" for the low level. For example, the low level for the first heating rate (β_1) was 40 K/hr while the high level was 100 K/hr. The samples were categorized as low (S_g < 25 m^2/g), medium (25 ≤ S_g ≤ 80 m^2/g) or high (80 m^2/g < S_g) surface area. The results are schematically illustrated in Fig. 7.

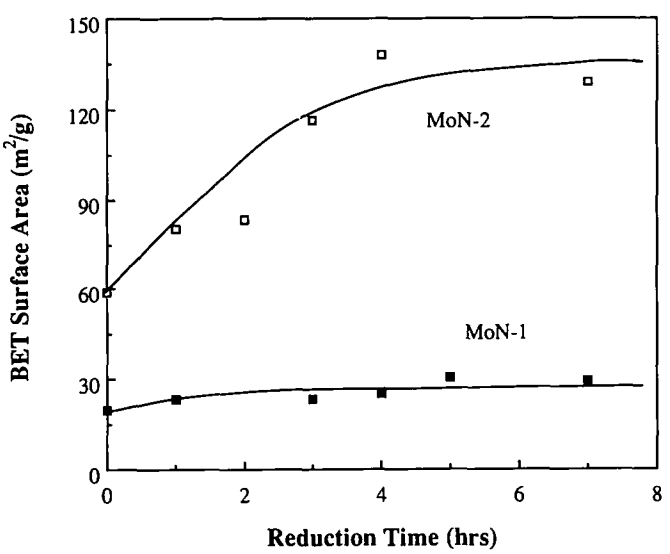

FIG. 6. Effect of reduction time on the BET surface areas of MoN-1 and MoN-2. These materials were reduced in H_2 at 673 K prior to the surface area measurements.

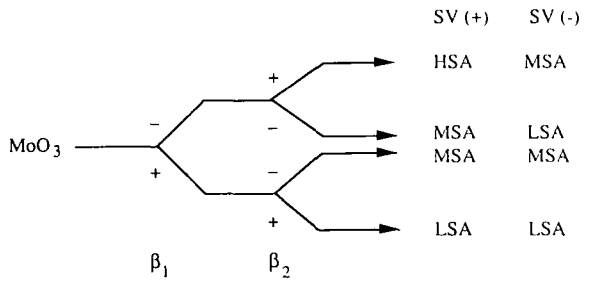

FIG. 7. Schematic illustrating the results of the temperature-programmed reaction of MoO_3 with NH_3 (SV represents the space velocity, and β_1 and β_2 represent the first and second heating rates, respectively). The low, medium, and high surface area catalysts are indicated by LSA, MSA, and HSA, respectively.

An unreplicated factorial design does not provide an independent estimate of the sample variance. It is, however, unlikely that all or none of the effects are significant, the latter because of the previously established effect of the space velocity. Therefore, the smallest effects shown in Table 4 were assumed to be random and independent normal variates. The estimated variance, s^2 = 207.5 for three degrees of freedom, was obtained from the effects for β_2, β_2SV and $\beta_1\beta_2$SV, and the $F_{1,3}$ ratios were constructed from this. The F ratio is a quantitative measure of the significance of the effect. The only effects significant at the 5% level ($F_{1,3:0.05}$ = 10.2) were SV and $\beta_1\beta_2$, that is the contribution of the effects of β_1 and β_1SV were buried in the experimental variance.

In every case examined, an increase in the space velocity caused an increase in the surface area, consistent with previous reports (2, 6). Changing the space velocity would affect the concentrations of gas-phase reactants and products at the solid surface. It has been suggested that the decrease in surface area with decreasing space velocity is due to the adverse effects of H_2O vapor produced during the reaction (6–8). Water vapor can cause hydrothermal sintering and the loss of surface area. The use of high

TABLE 4

Analysis of Variance of Factorial Design

Factor	Sum of squares	Effect	$F_{1,3}$ ratio
β_1	820.1	−20.3	4.0
β_2	210.1	10.3	—
SV	2426.1	38.3	14.1
$\beta_1\beta_2$	2278.1	−33.8	11.0
β_1SV	1770.1	−29.8	8.5
β_2SV	276.1	11.8	—
$\beta_1\beta_2$SV	136.1	−8.3	—

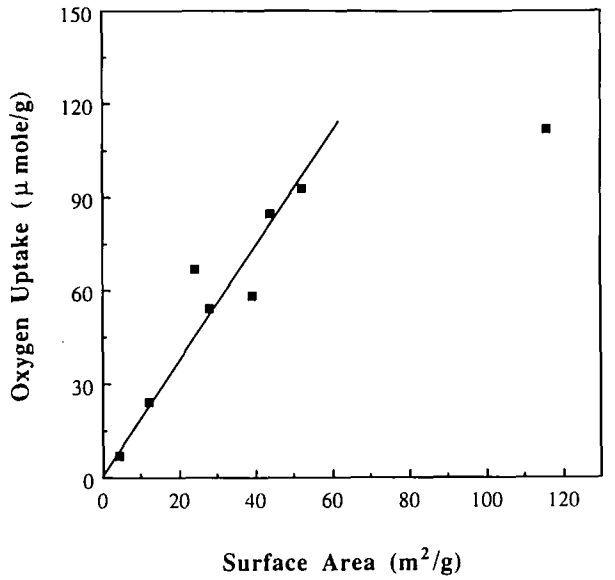

FIG. 8. Oxygen chemisorption on the molybdenum nitrides at 195 K as a function of the BET surface area. The materials were reduced in H_2 at 673 K for 3 hr.

space velocities would facilitate the removal of H_2O from the vicinity of the solid surface, thus reducing the potential for hydrothermal sintering. An alternative explanation is that H_2O adsorbs strongly at or diffuses slowly from the reaction interface, and channels the solid-state reaction away from the production of high surface area nitrides. This is analogous to product inhibition for a catalytic reaction. High space velocities reduce the potential for product inhibition.

The effects measured for the heating rates indicated that chemistry of importance in determining the molybdenum nitride surface area occurred during both heating segments. As the effect of the first heating rate potentiated (negatively) the effect of the second, the results also suggested the presence of two intermediates during the first and second heating segments. Intermediates during the first heating segment were H_xMoO_3 and MoO_2 based on the XRD results. Potential reaction intermediates during the second heating segments include γ-$Mo_2O_yN_{1-y}$, other molybdenum oxides, and molybdenum metal (given the phase constituents in MoN-5 and MoN-8). γ-$Mo_2O_yN_{1-y}$ is the oxynitride analog of γ-Mo_2N. Details concerning the influence of the heating rates on the reaction selectivities will be described.

As the Mo nitrides were employed as catalysts (10), we were also interested in their chemisorptive properties. For materials with surface areas up to $\approx$60 m^2/g, a proportionate number of chemisorption sites were exposed as new surface area was developed (Fig. 8). The highest surface area nitride had a somewhat lower relative O_2 uptake. The average number density was 0.11×10^{15} O_2/cm^2 based on the O_2 uptakes and BET surface areas. Assuming a Mo number density of $\approx 10^{15}$ Mo/cm^2 (valid for γ-Mo_2N and Mo), the average uptake was equivalent to a 21% surface coverage by atomic oxygen or about one oxygen atom for every 4–5 surface Mo atoms. Similar stoichiometries have been reported for H_2 (20) and CO (1, 5, 20) on Mo nitrides. These stoichiometries are considerably lower than those reported for chemisorption on Mo metal (21–23), and indicated that the intrinsic O : Mo stoichiometry for γ-Mo_2N is much less than unity, the surface consisted of patches of Mo and/or the surface was partially blocked by oxygen residue from the synthesis. The influence of residual oxygen was discounted based on X-ray photoelectron spectroscopic results (10). Bafrali and Bell (24) reported that the hydrogen saturation capacity for a Mo(100)–$c(2 \times 2)$N was 0.5 ML compared to a saturation coverage of 2.0 ML for a clean Mo(100) surface. This result suggests that molybdenum nitrides have lower O_2 chemisorptive capacities than Mo.

Solid-State Reaction Selectivity

A series of experiments was performed to further explore the intermediates generated during the molybdenum nitride synthesis. The reactions were carried out over the temperature ranges employed during the standard experiments: 623–723 K and 723–973 K. Products of the TPR of MoO_3 and H_xMoO_3 ($x \leq 0.34$) with NH_3 at varying

TABLE 5

Products of the Reactions of MoO_3 and H_xMoO_3 with NH_3

Solid reactant	Reaction conditions: T_{onset} (K)	T_{final} (K)	Heating rate (K/hr)	Solid products[a]
MoO_3	623	723	25	MoO_2, γ-$Mo_2O_yN_{1-y}$, MoO_3
MoO_3	623	773	25	MoO_2, γ-$Mo_2O_yN_{1-y}$
MoO_3	623	723	40	MoO_2, γ-$Mo_2O_yN_{1-y}$, MoO_3
MoO_3	623	773	40	MoO_2, γ-$Mo_2O_yN_{1-y}$
MoO_3	623	773	40[b]	H_xMoO_3, MoO_2, γ-$Mo_2O_yN_{1-y}$
MoO_3	623	773	85[b]	H_xMoO_3, MoO_3
MoO_3	623	723	100	MoO_2
MoO_3	623	773	100	MoO_2
H_xMoO_3	723	973	100[c]	MoO_2, γ-Mo_2N
H_xMoO_3	723	973	200[c]	γ-Mo_2N, MoO_2

[a] Listed in order of the height of the predominant peak for that phase in the XRD pattern.

[b] From *in situ* XRD results.

[c] The solid reactant was heated to T_{onset} in flowing He then switched to NH_3. For other experiments solid reactants were heated and cooled in NH_3.

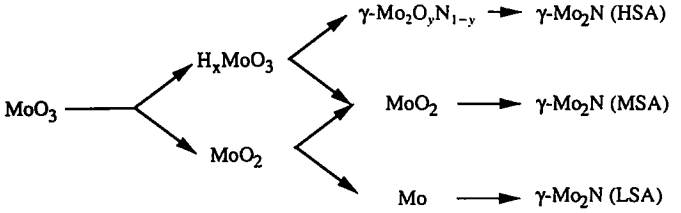

FIG. 9. Schematic illustrating the reaction pathways during the temperature-programmed reaction of MoO_3 with NH_3. The low, medium, and high surface area catalysts are represented by LSA, MSA, and HSA, respectively.

heating rates are listed in Table 5. We were unable to nitride the as-received MoO_2 at temperatures between 623 and 973 K using heating rates of 40–200 K/hr.

The reaction of MoO_3 at temperatures lower than 773 K produced H_xMoO_3, MoO_2, and γ-$Mo_2O_yN_{1-y}$. The oxynitride had a diffraction pattern very similar to that of γ-Mo_2N. Assignment of the product γ-$Mo_2O_yN_{1-y}$ was assisted by a report by Jaggers *et al.* (7) that temperatures greater than 773 K were necessary to produce γ-Mo_2N from MoO_3. The slower heating rate enhanced the selectivity to H_xMoO_3 and γ-$Mo_2O_yN_{1-y}$. The exact hydrogen content of the bronze could not be ascertained using X-ray diffraction, however, the pattern for the orthorhombic bronze ($x \leq 0.34$) is different from that for the monoclinic bronze ($x > 0.34$) (16).

The reaction of H_xMoO_3 ($x \leq 0.34$) with NH_3 produced medium and high surface area solids containing γ-$Mo_2O_yN_{1-y}$, MoO_2, and γ-Mo_2N. The reaction of H_xMoO_3 to γ-$Mo_2O_yN_{1-y}$ occurred near the transition between the heating segments (723 K), and was favored by the use of higher heating rates during the second heating segment.

DISCUSSION

We propose that the sequence illustrated in Fig. 9 describes the reaction pathways available during the TPR of MoO_3 with NH_3. The key to producing high surface area molybdenum nitrides from MoO_3 appeared to be channeling the reaction through H_xMoO_3 ($x \leq 0.34$) and γ-$Mo_2O_yN_{1-y}$ intermediates. The transformation of MoO_3 to H_xMoO_3 occurred at temperatures near 700 K in the presence of NH_3. At higher temperatures H_xMoO_3 was nitrided to produce γ-$Mo_2O_yN_{1-y}$ or decomposed to form MoO_2. While the reaction of H_xMoO_3 to γ-$Mo_2O_yN_{1-y}$ cannot be considered topotactic in the strict sense as has been suggested by Volpe and Boudart (8), it apparently occurs with a maintenance of gross morphology (pseudomorphism). The selectivity toward this reaction pathway was favored by using high heating rates as the temperature of the material was increased from 723 to 973 K. The oxynitride can be further nitrided to γ-Mo_2N by replacement of the lattice oxygen with nitrogen. This reaction is topotactic.

Molybdenum dioxide appeared to be the principal intermediate during production of the medium and low surface area catalysts. We believe that MoO_2, produced from MoO_3, could be nitrided to γ-Mo_2N or reduced to Mo. Nitrides produced directly from the metal typically possess low surface areas (5, 12, 13). Recall that molybdenum metal was present in the lowest surface area nitrides prepared in this study. We found no evidence for the production of δ-MoN from MoO_2, as was reported by Jaggers *et al.* (7).

Slow initial heating rates favored the reaction of MoO_3 to H_xMoO_3. The H_xMoO_3 phase can be formed via a topotactic reaction in which hydrogen is inserted between the loosely held double-thick layers of MoO_6 octahedra in MoO_3. Hydrogen is present as hydroxyl groups in H_xMoO_3 ($x \leq 0.34$) (25, 26). We suggest that when the heating rate is sufficiently slow, hydrogen from dissociated NH_3 has an opportunity to react with MoO_3 before it decomposes to MoO_2. Slow heating rates during the first heating segment would permit longer diffusion times and deeper penetration of hydrogen into the MoO_3 lattice. In the absence of sufficient amounts of hydrogen, competing reactions including the decomposition of MoO_3 to MoO_2 could occur. Fast heating rates over the temperature interval 723–973 K were also important for the production of high surface area molybdenum nitrides. Fast heating rates may favor the pseudomorphic nitridation of H_xMoO_3 to γ-$Mo_2O_yN_{1-y}$ by not permitting sufficient time for significant atom diffusion and morphological change. This would be analogous to the production of metastable and amorphous materials using very fast cooling rates.

CONCLUSIONS

A two segment heating program was employed to synthesize a series of molybdenum nitrides via the temperature programmed reaction of MoO_3 with NH_3. The results suggested that the synthesis of molybdenum nitride proceeded through a series of parallel reactions. Statistical analysis of the results indicated that the selectivity with respect to the surface area and phase constituents of the products depended on the space velocity individually and the heating rates combined. We concluded that the key to production of high surface area γ-Mo_2N was channeling the solid-state reaction through H_xMoO_3 ($x \leq 0.34$) and γ-$Mo_2O_yN_{1-y}$ intermediates. The reaction pathway from MoO_3 to H_xMoO_3 was favored by use of the high space velocity (17 hr^{-1}) combined with the low heating rate (β_1 = 40 K/hr). Reaction through other intermediates including MoO_2 resulted in the production of medium and low surface area molybdenum nitrides. Evidence of the maintenance of gross particle morphology during reaction

was observed for all the molybdenum nitrides but was most pronounced when comparing morphologies of the precursor MoO_3 and the highest surface area nitride. The maintenance of gross morphology is a condition that would lead to high surface areas given the significant increase in density on going from the oxide to the nitride.

Treatment of the passivated materials in H_2 at temperatures up to 673 K appeared to involve removal of oxygen from a near-surface oxynitride layer. Oxygen uptake following reduction, on catalysts with surface areas less than ≈ 60 m^2/g, varied linearly with the surface area. This corresponded to a site density of 0.11×10^{15} O_2/cm^2 or an O : Mo stoichiometry of approximately 1 : 5. The oxygen site density for the highest surface area nitride was somewhat lower than this value.

ACKNOWLEDGMENTS

The authors acknowledge financial support from the National Science Foundation (CTS-9158527) and the Shell Oil Company. We are also grateful for assistance from Kimberly Kolbert with the *in situ* X-ray diffraction and Christine Humphrey with the environmental scanning electron microscopy. Finally we acknowledge donation of the ESEM by the Amoco Corporation.

REFERENCES

1. Schlatter, J. C., Oyama, S. T., Metcalfe, J. E., III, and Lambert, J. M., Jr., *Ind. Eng. Chem. Res.* **27,** 1648 (1988).
2. Markel, E. J., and Van Zee, J. W., *J. Catal.* **126,** 643 (1990).
3. Choi, J.-G., Brenner, J. R., Colling, C. W., Demczyk, B. G., Dunning, J. L., and Thompson, L. T., *Catal. Today* **15,** 201 (1992).
4. Sajkowski, D. J., and Oyama, S. T., *Prepr.—Am. Chem. Soc. Div. Pet. Chem.* **35**(2), 233 (1990).
5. Volpe, L., Oyama, S. T., and Boudart, M., *in* "Preparation of Catalysts III" (G. Poncelet, P. Grange, and P. A. Jacobs, Eds.), p. 147. Elsevier, Amsterdam, 1983.
6. Oyama, S. T., Schlatter, J. C., Metcalfe, J. E., III, and Lambert, J. M., Jr., *Ind. Eng. Chem. Res.* **27,** 1639 (1988).
7. Jaggers, C. H., Michaels, J. N., and Stacy, A. M., *Chem. Mater.* **2,** 150 (1990).
8. Volpe, L., and Boudart, M., *J. Solid State Chem.* **59,** 332 and 348 (1985).
9. Günter, J., and Oswald, H. R., *Bull. Inst. Chem. Res. Kyoto Univ.* **53,** 249 (1975).
10. Brenner, J. B., Choi, J-G., and Thompson, L. T., submitted for publication.
11. Guttman, I., Wilk, S. S., and Hunter, J. S., "Introductory Engineering Statistics," 2nd ed. Wiley, New York, 1971.
12. Glemser, O., and Lutz, G., *Z. Anorg. Allg. Chem.* **264,** 17 (1951).
13. Toth, L. E., "Transition Metal Carbides and Nitrides." Academic Press, London, 1971.
14. Storms, E. K., *in* "Solid State Chemistry" (L. E. J. Roberts, Ed.), Vol. 10. Butterworths, London, 1972.
15. Cullity, B. D., "Elements of X-Ray Diffraction." Addison–Wesley, Reading, MA, 1978.
16. McClune, W. F. (Ed.), Powder Diffraction File; Alphabetical Index Inorganic Materials. International Centre for Diffraction Data, Swarthmore, PA 1991.
17. Colling, C. W., Choi, J-G., and Thompson, L. T., in preparation.
18. Choi, J.-G., Demczyk, B. G., and Thompson, L. T., accepted for publication in *Appl. Surf. Sci.*
19. Gregg, S. J., and Sing, K. S. W., "Adsorption, Surface Area, and Porosity," 2nd ed., p. 30. Academic Press, New York, 1982.
20. Ranhotra, G. S., Haddix, G. W., Bell, A. T., and Reimer, J. A., *J. Catal.* **108,** 24 (1987).
21. Riwan, R., Guillot, C., and Paigne, J., *Surf. Sci.* **47,** 183 (1975).
22. Felter, T. E., and Estry, P. J., *Surf. Sci.* **76,** 464 (1978).
23. Bowman, R. G., and Burwell, R. L., Jr., *J. Catal.* **63,** 463 (1980).
24. Bafrali, R., and Bell, A. T., *Surf. Sci.* **278,** 353 (1992).
25. Dickens, P. G., and Birtill, J. J., *J. Solid State Chem.* **28,** 185 (1979).
26. Slade, R. C. T., Halstead, T. K., Dickens, P. G., and Jarman, R. H., *Solid State Commun.* **45**(5), 459 (1983).